T H E   U N I V E R S I T Y   O F   M I C H I G A N

COLLEGE OF ENGINEERING
Cast Metals Laboratory

Progress Report No. 1

MICROSTRUCTURE CONTROL IN MOLYBDENUM DUCTILE IRONS

D. R. Askeland
P. K. Trojan

ORA Project 31084

under contract with:

CLIMAX MOLYBDENUM COMPANY OF MICHIGAN
ANN ARBOR, MICHIGAN

administered through:

OFFICE OF RESEARCH ADMINISTRATION   ANN ARBOR

November 1968

TABLE OF CONTENTS

LIST OF ILLUSTRATIONS

SUMMARY

Several combinations of nodularizers, post inoculants, and metal chemistry have indicated a 4% Mo; 4% Si; 1% Al ductile cast iron to be somewhat insensitive to process variation. The present report on research progress also evaluates the effects of cooling rate and heat treatment response on the carbide-graphite shape, amount, and distribution. These results suggest further work in correlation of microstructure with aluminum content and processing treatment at the 2% Mo level. Complimentary work in solid state induced graphitization should help in understanding the eutectic carbide-vermicular graphite interrelationships.

INTRODUCTION

Recent results on molybdenum-containing ductile cast irons have shown some difficulty with control of graphite shape and with the propensity of carbide.[1] The present research was therefore initiated to evaluate the processing variables which affect the graphite-carbide shape, quantity, and distribution. With a nominal chemistry of 3.0 C; 4.0 Si; 0.30 Mn; 1.0 Al; and 2.0 to 4.0 Mo the following variables are to be considered:

1. Nodularizer type
2. Post inoculant type
3. Cooling rates (chill surface to 3" sections)
4. Heat treatment response
5. Chemistry variations

The present progress report summarizes the results of the investigation over the first three months of the research.

EXPERIMENTAL PROCEDURE

Previous work at the Cast Metals Laboratory has resulted in a processing procedure for ductile cast iron which would allow critical evaluation of variables such as outlined above.[2] The general procedure is given below:

MELTING

The raw materials used in the investigation are given in Table I. The pig iron, high purity silicon, electrolytic manganese, ferro-molybdenum, and Armco iron are charged to a 3000-cycle, 115-lb capacity, alumina-lined induction furnace. Since all of the material cannot be charged at once, some pig iron is withheld until the initiation of melting, at which time the remainder is added to the partially molten bath.

When the metal is completely molten, 2 lb of CaC_2 (nut size) is added as a protective cover for the melt. The power is turned off when the melt reaches 2900°F and the CaC_2 is removed. The aluminum addition is then made by plunging pure ingot. Upon cooling to 2750°F, the metal is treated with the magnesium alloy in an open ladle by the transfer technique. The post inoculant is added to the furnace (0.50% Si added) and the metal is poured back into the furnace which insures excellent mixing and solution of the post inoculant.

Finally the metal is tapped into a teapot ladle for pouring.

MOLDING AND POURING PROCEDURES

The molds poured and their descriptions are listed below:

Casting No.	Mold Material	Comments	
1	6 mm bore Vycor	Chem sample before nodularization	
2	6 mm bore Vycor	Chem sample after nodularization	
3	6 mm bore Vycor	Chem sample after post inoculation	
4	Dry sand	1/4" y-block	in one flask Fig. 1
5	Dry sand	1/2" y-block	
6	Dry sand	1" y-block	
7	Dry sand	1/4" y-block	in one flask Fig. 1
8	Dry sand	1/2" y-block	
9	Dry sand	1" y-block	
10	Core sand-graphite	Chem sample—1" dia coupons	
11	Dry sand	3" y-block	
12	Core sand	Chill wedge	Fig. 2
13	Core sand	Chill wafer	
14	Steel	1" dia round	

The dimensions of the y-block sections are shown in Fig. 1. The sand composition used for the y-blocks was 4% western bentonite, 0.3% dextrin, 0.3% wood floor, and 3.5% water. The molds were dried for 12 hours at 300°F before being poured. The chill wafer was poured against a graphite plate while the chill wedge cooled most rapidly at the acute angle of the triangular cross-section (Fig. 2). The round chill was cast in a steel mold which provided a very rapid cooling rate.

The entire set of castings (nos. 4-14) were poured in less than 60 sec. The pouring temperature for all heats was controlled from 2550-2600°F. Temperature indication was with an immersion Pt-Pt 10% Rh thermocouple.

RESULTS AND DISCUSSION

The chemical analyses and scope of several heats are shown in Table II. All heats were run at the 4% molybdenum level in the hope that control of graphite and carbide would be more acute at the higher molybdenum content. Since the major control requirement is based upon microstructural occurrences, a 1/2" y-block was sectioned from each heat as a quick check on the graphite-carbide distribution.

The microstructure will, of course, vary as the cooling rate is varied. It was therefore of interest to know the exact cooling rates for the y-block sections. Thermocouples were placed at the thermal center of each section as shown in Fig. 1. The corresponding cooling curves are given in Fig. 3. The solidification time range was actually very broad; from less than 1/2 min in the 1/4" y-block to 15 min in the 3" y-block. The cooling curves reported in Fig. 3 were obtained for heat no. 9.

The discussion of the microstructural variations has been divided into the following categories for ease of data presentation.

1. Section Sensitivity
2. Effects of Nodularizer and Post Inoculant
3. Effect of Metal Chemistry
4. Heat Treatment Response

1. Section Sensitivity

The extreme differences in cooling rates as shown in Fig. 3 should indicate variations in the microstructure. An example of the section size dependency is shown in Figs. 4 and 5. Both the 1/4" and 3" sections showed carbide and decayed graphite in conjunction with the desired spheroidal graphite shape. Of course the nodule count or graphite nucleation sites are seen to be lower in the 3" section. Also the amount of nonspheroidal or decayed graphite is greater in the larger section.

It is a well known phenomenon that processing variables which effect graphite size will also effect the carbide size. Therefore it should be noted that the size of the carbide is also greater in the large 3" section. The occurrence of the upgraded graphite flakes or vermicular graphite in these heavier sections is possibly due to the graphitization of the larger carbides.

2. Effects of Nodularizer and Post Inoculant

Figures 4 and 5 are quite representative of all heats poured (Table II). All combinations of nodularizer and post inoculant resulted in carbide, spheroidal graphite, and vermicular graphite for all section sizes. It is of interest that even though carbide could not be suppressed at the 4% Mo level, graphite could also not be suppressed (Fig. 10 illustrates graphite presence next to a chilled surface).

A somewhat extreme change in nodularizer and post inoculant can be seen by comparison of Figs. 4 and 6. Although there appears to be some difference between the two microstructures, the same graphite-carbide shapes considered to be detrimental occur in both structures. It is interesting to note that mold inoculation in the form of 0.02% Si as 85% FeSi in the bottom of the y-block sections also did not have an effect on the as-cast microstructure.

3. Effects of Metal Chemistry

The stabilization of carbide by magnesium has been well documented in the literature. This appears to hold true for the primary solidification product, however the effect has not been well established for the occurrence of carbide over graphite as the eutectic product. In order to determine the carbide stabilization by magnesium, two special heats were conducted. Figure 7 shows the microstructure of a 1/2" section with no magnesium added while Fig. 8 illustrates the result of undertreatment with magnesium (0.01 Mg residual). In both cases the amount of carbide has not changed significantly. Of course the degree of graphite nodularity is seen to be less than in the previous figures. The higher magnification used in Fig. 7 is particularly interesting in that the primary graphite appears to have stable eutectic carbide in very close association with no tendency for carbide dissociation.

A theory has also been put forth that magnanese content might control the occurrence of the carbide. Figure 9 has been obtained for a 1/2" section which contained half of the normal manganese content (0.17 vs. 0.35). Again the microstructure is very similar to the normal graphite-carbide distribution as shown in the previous figures.

It would therefore appear that the chemistry variations above do not change the incidence rate of the eutectic carbide. They may however change the stability of carbide as indexed by a response to a heat treatment destruction of the carbide.

4. Heat Treatment Response

It should be apparent from the preceding discussion that the eutectic carbide is difficult to destroy through normal processing variation. Due to the insensitivity, a series of solid state heat treatments were conducted to test the carbide thermal stability. Two temperatures, 1750°F and 1850°F, were selected for the microstructural comparison. The specimens were taken from heat no. 3 (Table II) and consisted of chill wafer sections at the chill surface and 3/4" from the chill (Fig. 2). After holding each specimen for 2 hours at temperature, the samples were given an air quench.

The series of as-cast, 1750°F, and 1850°F microstructures at the chilled surface are shown in Figs. 10-12. Although the amount of carbide decreased slightly between the as-cast and 1750°F treatment, the added 100°F in going to 1850°F showed a much greater decrease (unfortunately the low magnification of 100X does not completely describe this effect). On the other hand the disappearance of carbide must by accompanied by: solid solution of carbon, growth of existing graphite, and/or nucleation of more graphite.

Figures 10-12 appear to indicate that the amount of flake or vermicular graphite decreases as the carbide decreases. Since the diffusion distances are short when the nodule or eutectic cell count is high, it is difficult to believe that more graphite is nucleated during heat treatment, although this is not immediately apparent from the microstructures. The shape change in graphite is however difficult to explain at this time since the possibilities range from solution and reprecipitation of graphite to coalescence of the existing graphite.

Figures 13-15 show the effect of heat treatment on samples cut at 3/4" from the chill. The low nodule count and larger eutectic cell size are, of course, striking when compared to Figs. 10-12. Again there may possibly be some loss in the quantity of decayed graphite as the material is heat treated. However it also appeared that the amount of graphite decreases, which was not immediately evident in Figs. 10-12.

CONCLUSIONS AND RECOMMENDATIONS

The above discussion of microstructural variation in 3.25 C; 4.0 Si; 1.0 Al; 4.0 Mo nodular cast iron permits the following general conclusions:

1. Eutectic carbide, nodular graphite, and vermicular graphite occur in all sections from a chill surface to a 3" y-block.

2. Several combinations of nodularizer, post inoculant, manganese content, and residual magnesium indicate the microstructure to be insensitive to

these processing variables. In each case undesirable graphite shape and eutectic carbide were present.

3. The response of the microstructure to heat treatment indicates possible graphite solution in more slowly cooled sections and loss of decayed graphite shapes in the rapidly cooled sections as the heat treatment temperature is increased.

These conclusions represent the initial phases of the research. Below are several recommendations for further work of which all phases are presently in progress.

1. Determine the effect of aluminum on the graphite-carbide distribution at the 2 and 4% molybdenum levels.

2. With 1% Al present, evaluate the effects of nodularizer, post inoculant, and section size in the 2% molybdenum alloy.

3. Evaluate further the effect of heat treatment upon the graphite-carbide stability at the 4% Mo level. 1/4" and 3" y-block sections will be used as extremes in this study.

BIBLIOGRAPHY

1. Sponseller, D. L., Scholz, W. G., and Rundle, D. F., "Development of Low-Alloy Ductile Iron for Service at 1200-1500°F," Trans. Amer. Fndrymn's Soc., 76, 353-368 (1968).

2. Trojan, P. K., Bargeron, W. N., and Flinn, R. A., "The Evaluation of Nodularizers and Post Inoculants for Ductile Iron," Trans. Amer. Fndrymn's Soc., 75, 611-624 (1967).

TABLE I

CHEMICAL ANALYSES OF RAW MATERIALS

Material	% C	% Si	% Mn	% P	% S	% Mg	% Mo	% Al	% Sr	% Ni	% Ce	Others
Pig Iron A	4.25	—	.08	.022	.015	—	—	—	—	—	—	.020 Ti
Pig Iron B	4.55	.60	.20	.017	.016	—	—	—	—	—	—	—
Armco	.015	.003	.03	.005	.025	—	—	—	—	—	—	—
CeMgFeSi	—	48.2	—	—	—	8.60	—	.93	—	—	.51	1.20 Ca
NiMg	—	31.2	—	—	—	14.65	—	—	—	50.1	—	.06 Cu
MgFeSi	—	46.5	—	—	—	8.49	—	.75	—	—	—	1.48 Ca
Al Mg	—	—	—	—	—	14.47	—	Rem.	—	—	—	—
75% FeSi	—	75.94	—	—	—	—	—	1.30	—	—	—	1.05 Ca
SrFeSi	—	69.63	—	—	—	—	—	.85	.88	—	—	.09 Ca
FeMo	.03	.45	—	.05	—	—	62.0	—	—	—	—	—
Al Metal	—	—	—	—	—	—	—	99.9	—	—	—	—
Si Metal	—	98.98	—	—	—	—	—	.09	—	.01	—	.54 Fe
Elec. Mn	—	—	99.95	—	.023	—	—	—	—	—	—	.20 O
BaSi	—	50.0	—	—	—	—	—	—	—	—	—	Rem. Ba

TABLE II

HEAT CHEMISTRIES AND PURPOSE

Heat No.	Nodularizer	Post Inoculant	% C	% Si	% Mn	% Mo	% Al	% Mg	Comments
2	MgFeSi	75% FeSi	3.16	4.28	.29	4.10	1.22	.041	
3	CeMgFeSi	75% FeSi	3.22	3.50	.46	4.20	1.37	.042	
4	CeMgFeSi	SrFeSi	3.20	4.26	.39	3.96	1.06	.031	
5	NiMg	SrFeSi	3.32	4.23	.37	4.10	1.03	.033	
6	MgAl	SrFeSi	3.49	4.03	.33	4.12	0.91	.031	
7	CeMgFeSi	BaSi*	3.27	4.11	.37	4.20	1.00	.033	
8	None	75% FeSi*	3.52	4.49	.35	3.88	.74	None	No Mg added
9	MgFeSi	75% FeSi*	3.48	4.34	.30	3.75	.84	.011	Low Mg heat
10	CeMgFeSi	75% FeSi*	3.66	4.17	.17	3.75	.90	.024	Low Mn heat

Note: Sulfur and phosphorus less than 0.020 for all heats.

*0.02 Si added as 85% FeSi (-28 +140 mesh) to molds 7, 8, and 9.

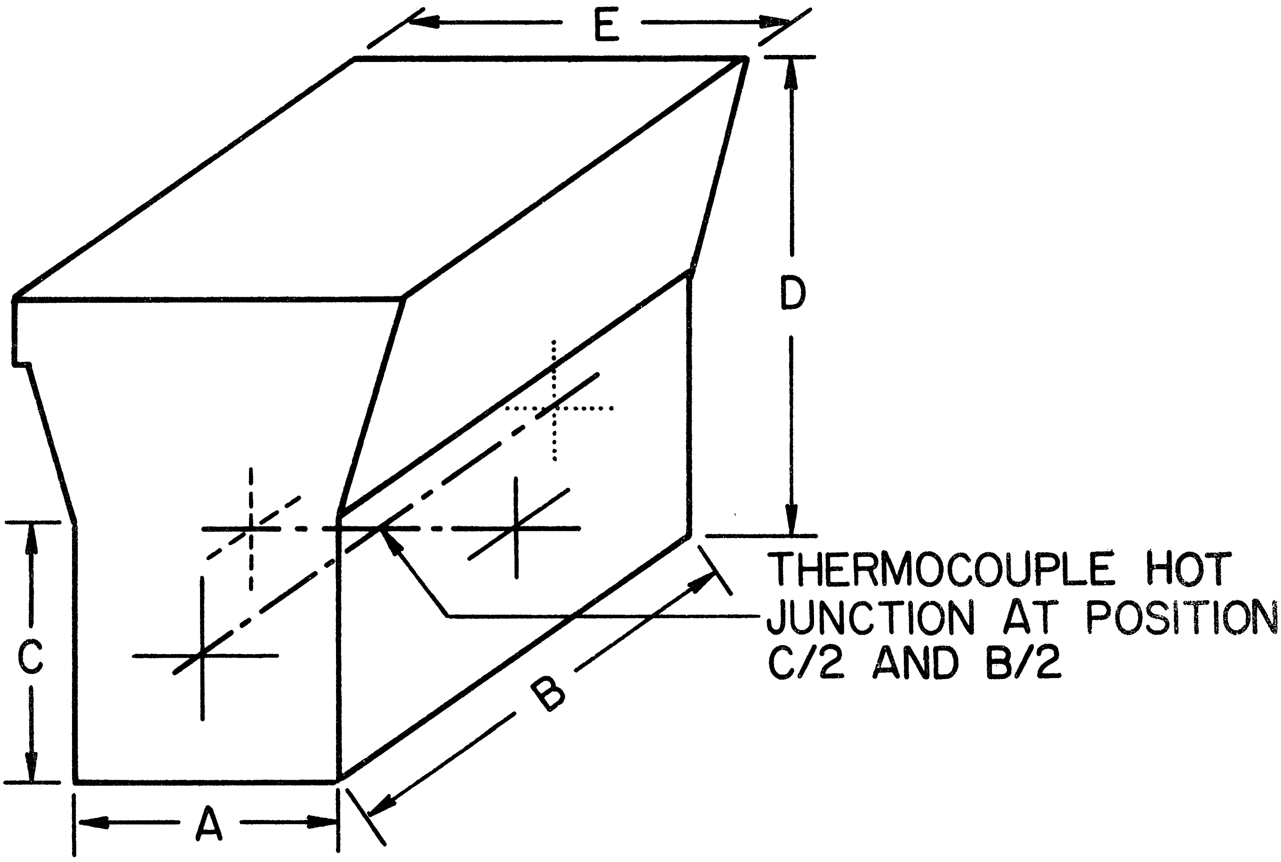

y-BLOCK (INCHES)	A (IN.)	B (IN.)	D (IN.)	C (IN.)	E (IN.)
3	3	6	5 1/2	2 1/2	4 3/4
1	1	6	4 1/4	1	2
1/2	1/2	6	3 1/2	1	1 1/2
1/4	1/4	6	2	1/2	1 3/4

Fig. 1. y-block design, dimensions, and thermocouple placement.

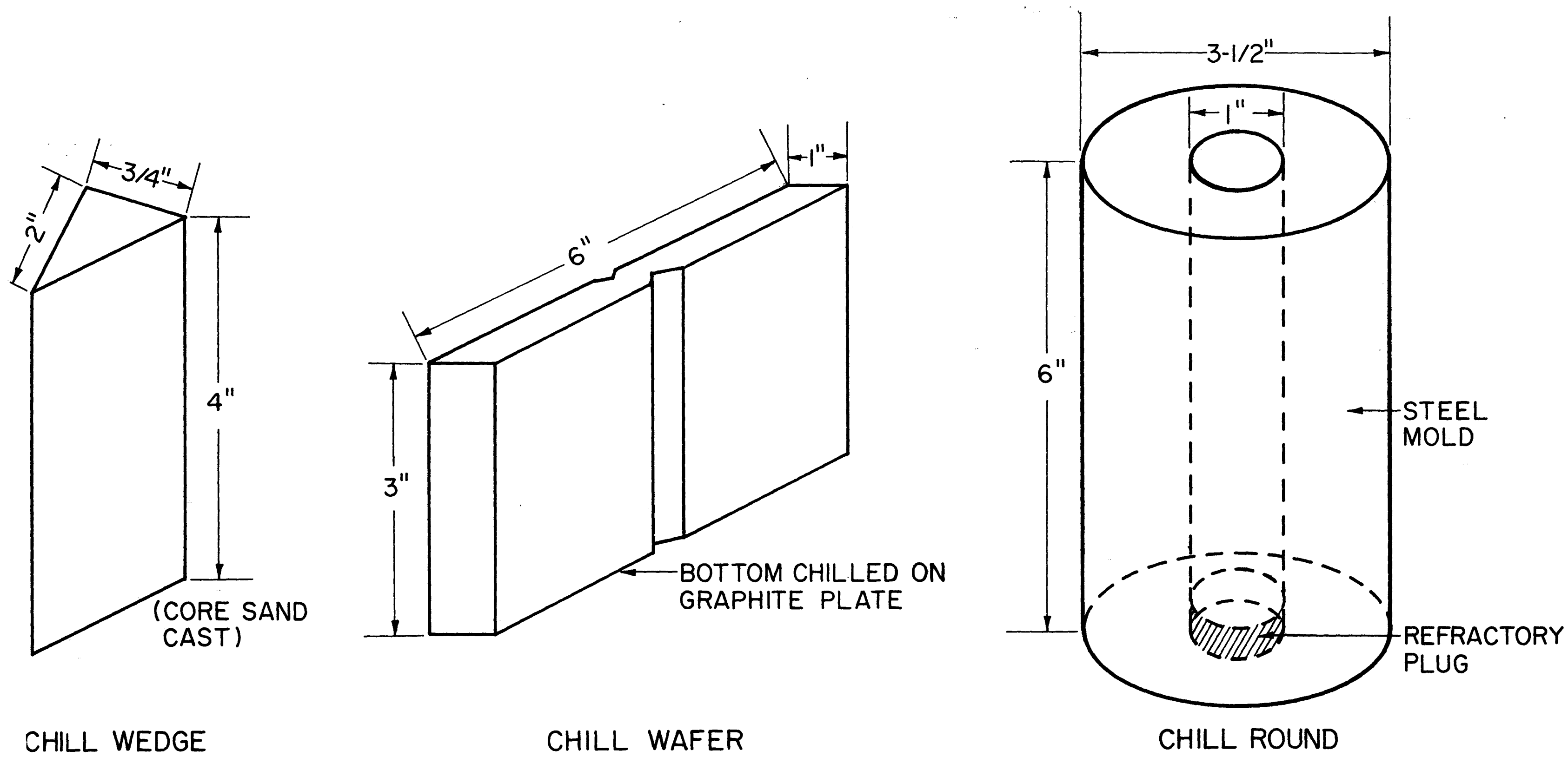

Fig. 2. Chill wedge, wafer, and round dimensions and design.

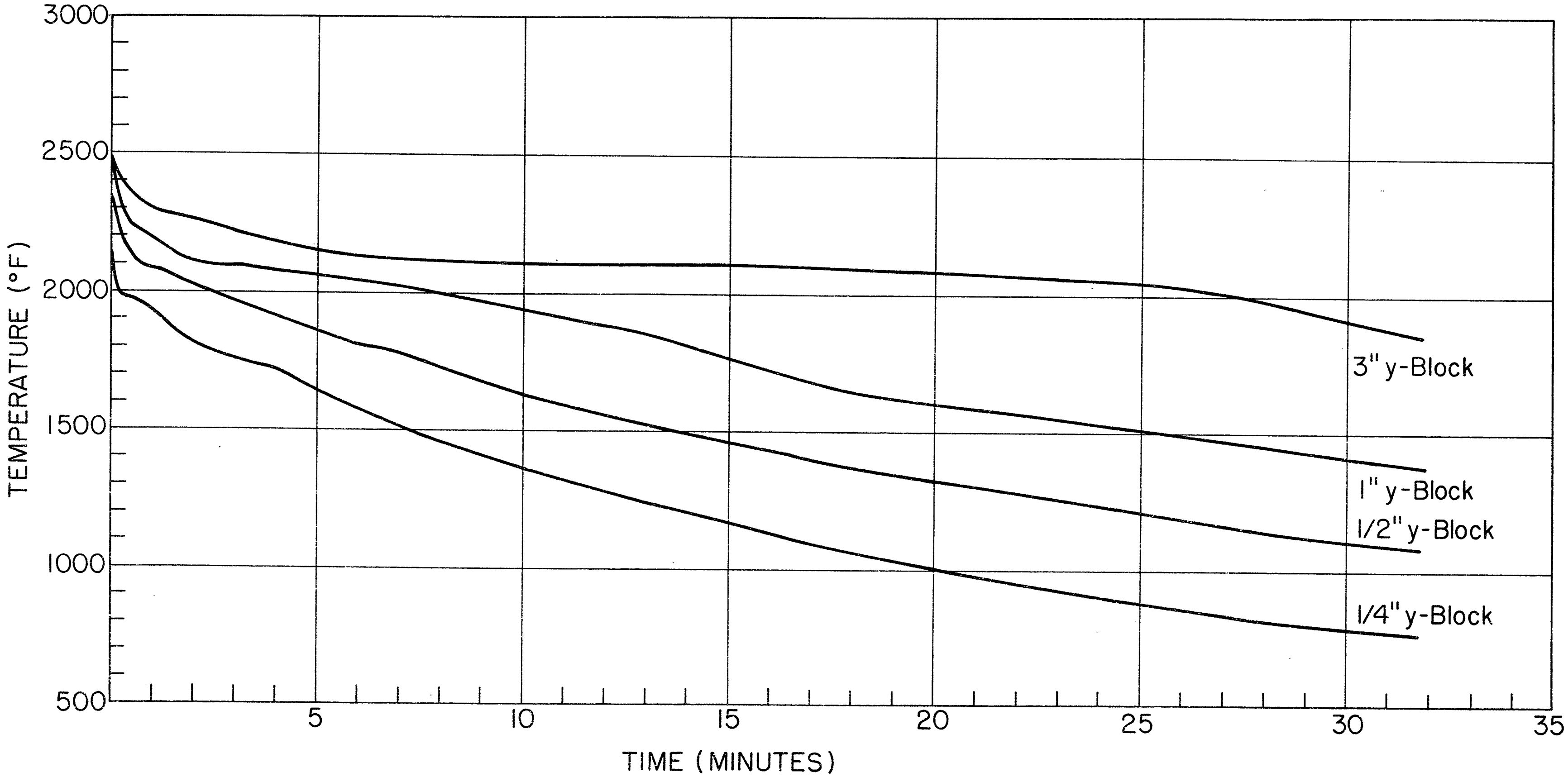

Fig. 3. Cooling curves for y-block sections.

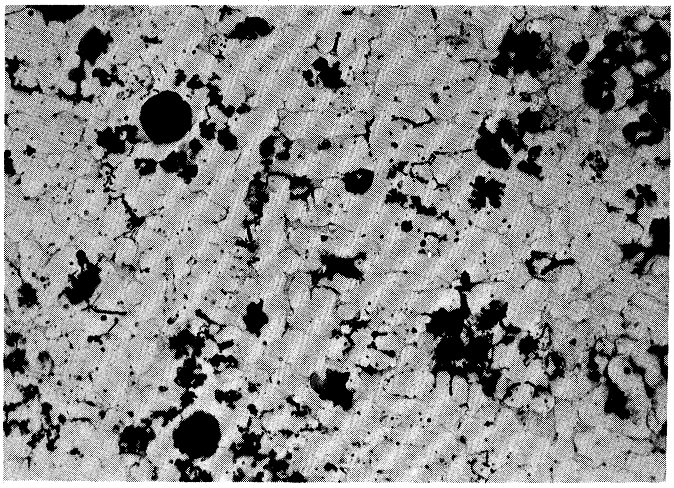

Fig. 4. 100X. 1/2" y-block; CeMgFeSi; 75% FeSi.

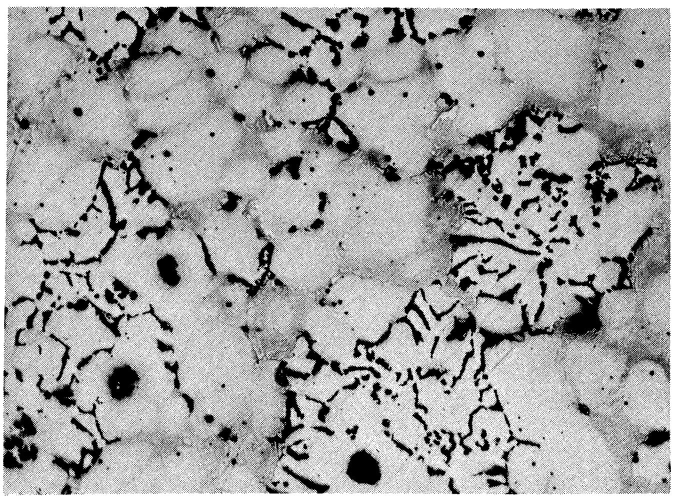

Fig. 5. 100X. 3" y-block; CeMgFeSi; 75% FeSi.

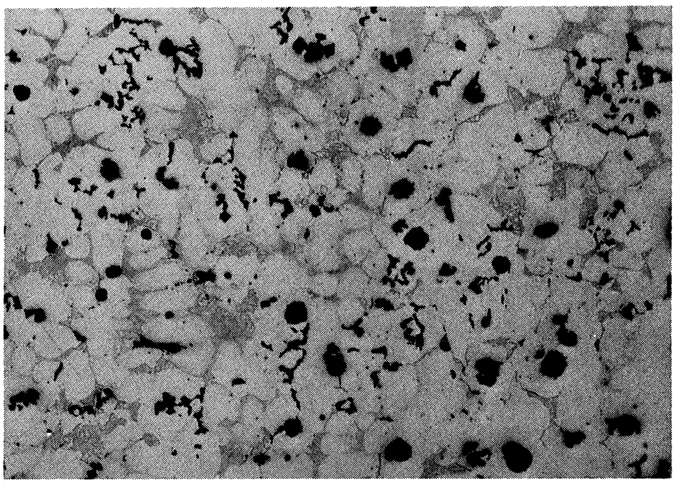

Fig. 6. 100X. 1/2" y-block; NiMg; SrFeSi.

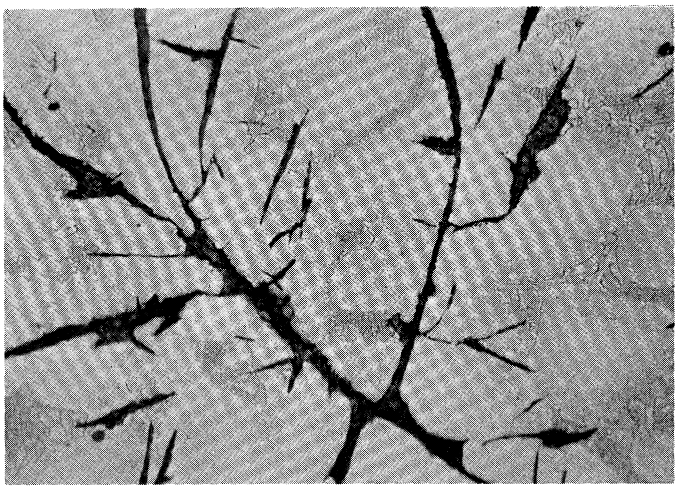

Fig. 7. 500X. 1/2" y-block; no magnesium added; 75% FeSi.

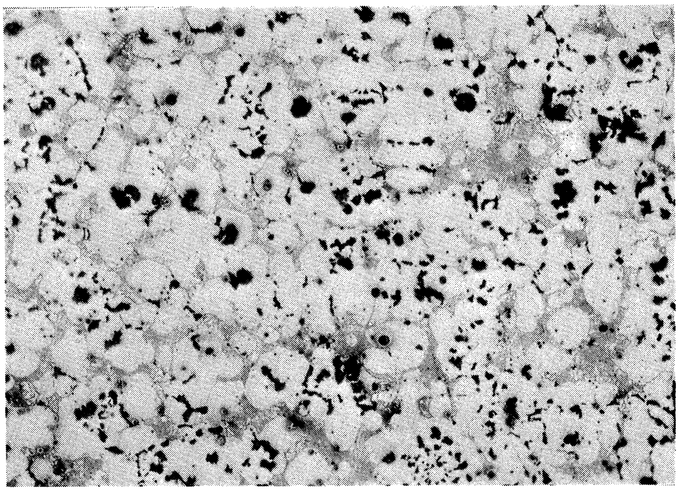

Fig. 8. 100X. 1/2" y-block; MgFeSi; 75% FeSi; 0.011 residual magnesium.

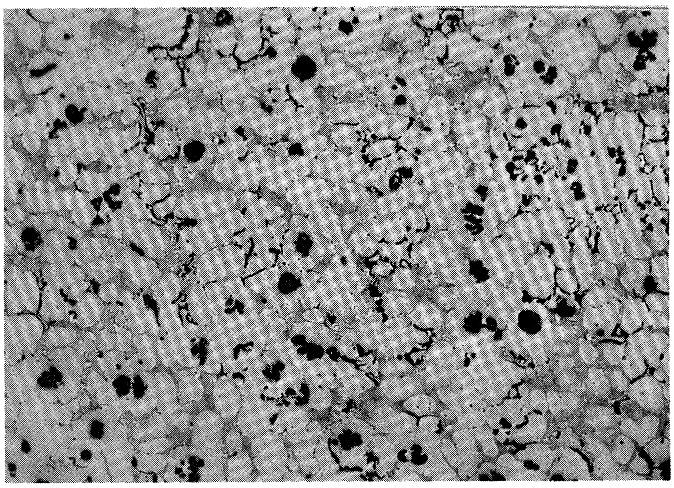

Fig. 9. 100X. 1/2" y-block; CeMgFeSi; 75% FeSi; low manganese content (0.17%).

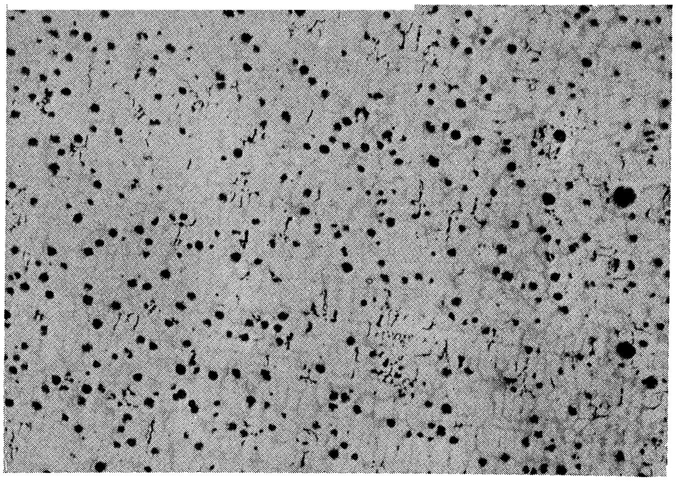

Fig. 10. 100X. CeMgFeSi; 75% FeSi; surface of chill wafer; as-cast.

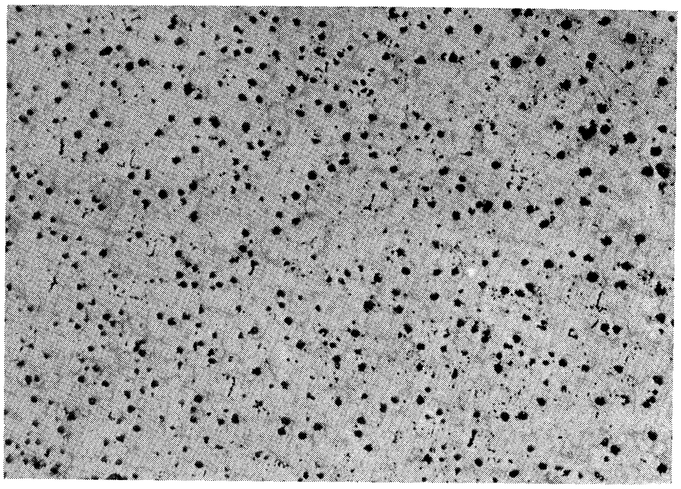

Fig. 11. 100X. Surface of chill wafer in Fig. 10 after 2 hours at 1750°F.

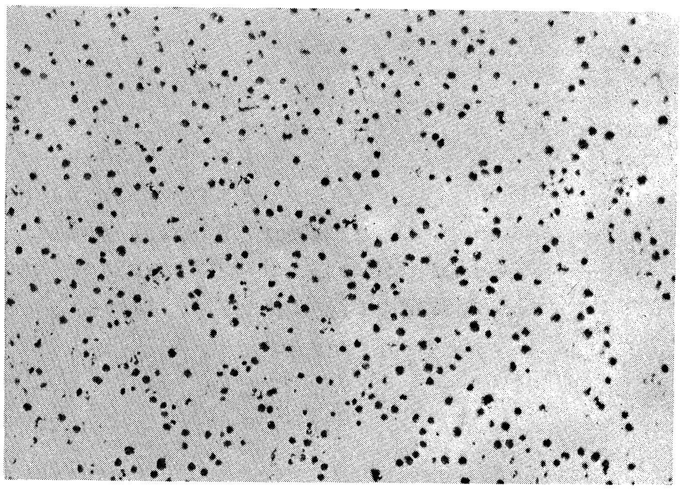

Fig. 12. 100X. Surface of chill wafer in Fig. 10 after 2 hours at 1850°F. (Carbide is still present, however sample is unetched.)

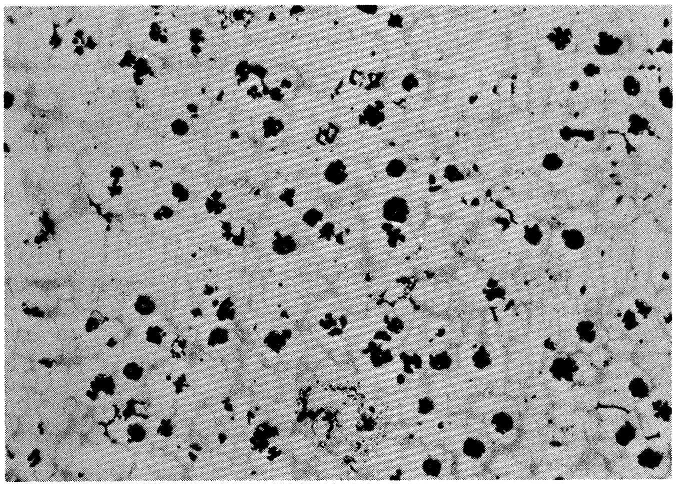

Fig. 13. 100X. CeMgFeSi; 75% FeSi; 1" from chill wafer surface; as-cast.

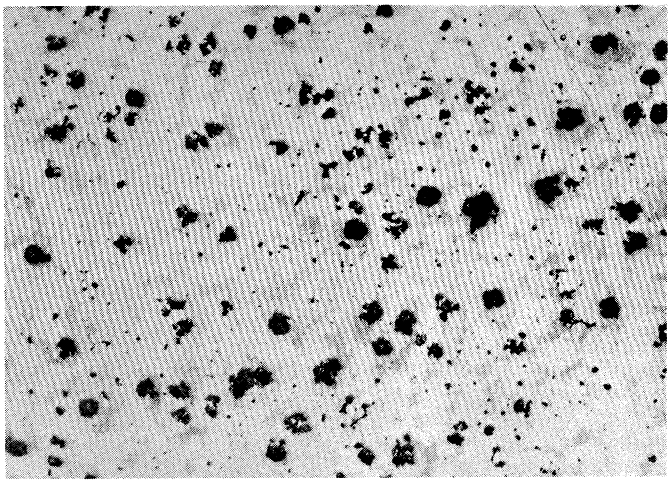

Fig. 14. 100X. 1" from chill wafer surface after 2 hours at 1750°F.

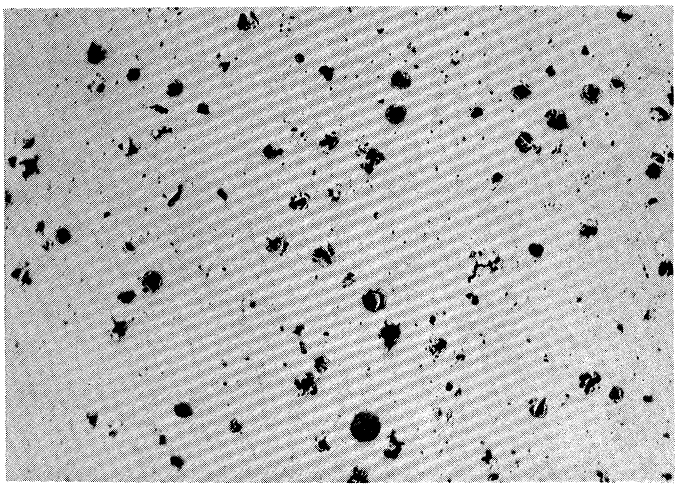

Fig. 15. 100X. 1" from chill wafer surface after 2 hours at 1850°F. (Again not all of the carbide has been destroyed.)